INSTITUTE FOR NUCLEAR STUDY
UNIVERSITY OF TOKYO
Tanashi, Tokyo 188
Japan

INS-Rep.-823
April 1990

Festschrift in honour of Torleif Ericson's 60th Birthday

REAL-PION STATES FORMED BY VIRTUAL-PION BEAM: NEW FAMILY OF NUCLEAR EXCITED STATES

Toshimitsu Yamazaki
Institute for Nuclear Study, University of Tokyo
Tanashi, Tokyo 188, Japan

INS-Rep.-823
April 1990

Festschrift in honour of Torleif Ericson's 60th Birthday

REAL-PION STATES FORMED BY VIRTUAL-PION BEAM: NEW FAMILY OF NUCLEAR EXCITED STATES

Toshimitsu Yamazaki
Institute for Nuclear Study, University of Tokyo
Tanashi, Tokyo 188, Japan

Deeply bound pionic states are discussed from various points of view; highly excited nuclear states as a cluster family of pionic bound states, Σ atom/Σ hypernuclei, halo-like density distributions, virtual pion beam to produce pionic states, *etc.*

1. INTRODUCTION: HYPERNUCLEI AND PIONIC NUCLEI

Pionic atoms have yielded fruitful information on the interaction of pions with nuclei since early days [1]. The levels and widths were fitted to the pion-nucleus optical potential of the Ericson-Ericson type [2] and by now the potential parameters are well established [3]. Exotic atoms which are composed of a strongly-interacting negative particle and a nucleus are characterized by level shifts and absorption widths near the "last orbitals", where the x-ray cascades stop continuing. Recent experimental studies have revealed that these levels and widths cannot be represented by a single optical potential [4,5]. This phenomenon, called "anomaly", has been given various theoretical considerations, but no definite explanation has been reached. This issue leads us to a natural question as to whether such a deviation between experiment and theory increases for the next inner orbitals or

not. Unfortunately, no orbitals inside the last orbitals have ever been accessed experimentally in pionic x-ray spectroscopy for obvious reason.

A similar situation exists in the case of Σ atoms and Σ hypernuclei. The Σ hyperon is strongly absorbed by a nucleus through the $\Sigma N \rightarrow \Lambda N$ conversion. This process is expected to contribute to an absorption width as broad as 20 MeV. In general, a Σ hypernucleus is regarded as an excited state of Λ hypernucleus with excitation energy of around 80 MeV. Whether Σ bound states exist with narrower widths or not has been a very intriguing problem, but it remains still unsettled.

Recently, Hayano *et al.* [6] found a positive evidence for the bound state of ${}^4_\Sigma$He with $S = 0$ and $I = 1/2$ from a ^{4}He (stopped K^-, π^-) spectrum, as shown in Fig.1, though no bound state has been identified in other nuclei. This bound state had been predicted by Harada *et al.* [7], who used the two-body hyperon-nucleon interactions which are compatible with the Nijmegen D potential. This state is interpreted as a kind of "halo state", namely, the Σ particle is loosely bound by a wine bottle-type potential, as shown in Fig.2. The central repulsive core is a result of the hard core in the hyperon-nucleon interaction. Because of the smaller overlapping of Σ^- with the nuclear core the absorption width is reduced to 4 MeV. This is the reason why the ${}^4_\Sigma$He bound state exists with a narrow width.

For Σ^- hypernuclei Yamazaki *et al.* [8] considered Coulomb-assisted hybrid bound states. Namely, the long-range Coulomb attraction accomodates bound states which are "half nuclear" and "half atomic", as shown in Fig.3. Since the nuclear absorption represented by an imaginary potential $iW(\vec{r})$ takes place only inside the nucleus, the width of such a "hybrid" level is reduced as given by

$$\Gamma_{n\ell} = -\int \rho_{n\ell}(\vec{r}) W(\vec{r}) d\tau, \quad (1)$$

where $\rho_{n\ell}(\vec{r})$ is the density distribution of a Σ^- state with quantum numbers (n, ℓ).

The extreme "atomic" limit corresponds to Σ atoms, and the extreme "nuclear" limit is called Σ hypernucleus. They are the two limiting cases of the Σ^- bound system, but are continuously connected; there is no essential distinction between Σ^- atoms and Σ^- hypernuclei. It is interesting to note that Myint, Tadokoro and Akaishi [9] predicted the presence of a repulsive barrier for Σ^- near the nuclear surface which divides the inner region and the outer region. Inside, the bound state is too broad to be observed as a discrete state, while outside, the bound states are "Coulomb assisted" narrow states. Such states are subject to future experimental investigation [10].

In the field of hypernuclear spectroscopy tremendous efforts have been put into the identification of Σ hypernuclei. In great contrast, however, there has been no effort to identify "pionic nuclei", neither experimentally nor theoretically. People seem to stop thinking about the inner world of pionic bound states, as if they believe that the inner states are *non-existing*. It is clear that the termination of pionic atom cascades by pion absorption has nothing to do with the existence of inner bound states. The criteria for the existence of a bound state is that the level width be smaller than the typical level spacing, namely,

$$\Gamma_{n\ell} \leq \Delta E. \tag{2}$$

The width could be as much as a few MeV. On the other hand, the width of the last orbital is of the order of the x-ray transition probability, namely,

$$(\Gamma_{n\ell})_{\rm last} \sim \Gamma_{\rm rad}, \tag{3}$$

which is, typically 10 keV or so, orders of magnitude smaller than $\Gamma_{n\ell}$. In spite of the popularity of pion-nuclear physics, its physics scope was smaller than the less

popular hypernuclear physics.

Pionic states and Σ hypernuclear states are equally characterized as special kinds of nuclear excited states, where a new degree of freedom of "real" pion or "real Σ" emerges. If they are loosely bound, their widths become small enough to be observed as discrete states. For a negatively-charged particle like π^- and Σ^- the long-range Coulomb attraction helps accomodate rather sharp bound states up to the threshold. They constitute a new family of states formed by a "particle cluster" which is unstable inside the nucleus. See Fig.4 for this generalized diagram of nuclear excited states.

According to the famous phrase of Ikeda [11], a cluster is "externally weak and internally strong". As far as a cluster is loosely bound, it keeps its free identity, but as it is tightly coupled, the cluster is dissolved into a nuclear medium as a broad state, and loses its identity more and more; it becomes "externally strong and internally weak". The cluster is best revealed just below the threshold of the cluster emission (in the present case, below the π^- emission threshold). Deeper states lose the cluster character more.

If pionic bound states are found, they will give a very important information about the behavior of real pions in nuclear medium [12]. They may be related to the question as to *what is pion* and *to what extent the pion preserves its free identity (mass, size) in nuclei* [13]. So far, investigations have been done in the case of baryons [14] in connection with the EMC effect [15], but not for mesons. In view of such exciting possibilities we tried to attack the problem both theoretically and experimentally.

2. STRUCTURE OF PIONIC NUCLEI

Toki and Yamazaki [16] and then Toki *et al.* [17] started systematic theoretical studies of the structure and formation of deeply bound states of π^- in heavy nuclei.

Surprisingly, they found that the deeply bound π^- states have narrow widths, if the known pion-nucleus optical potential is used. They also considered how such deeply bound π^- states can be produced.

The level structures of π^- in ^{90}Zr and ^{208}Pb are shown in Fig.5. The widths are all narow. How can this fact be reconciled with the large absorption potential of π^-? The answer is simple; the pion-nucleus potential causes a repulsive core which is surrounded by an attractive Coulomb potential, as shown in Fig.6. The calculated densities of the first three states (1s, 2s and 2p) are shown in the figure. They are pushed outward due to the central repulsion. Thus, the deeply bound π^- states form "pion halo". The halo-like π^- states are expected to have narrow widths.

This is even more so, if the nuclear surface has a neutron skin or halo, since the neutron part without proton density does not contribute to π^- absorption. This mechanism for narrow π^- states was once considered by Friedman and Soff [18] for the π^- ground state in heavy and superheavy nuclei. They pointed out that the quasi-stable π^- ground state could be collapsed when the nuclear charge increases beyond a critical value ($Z \geq 100$), because the strong Coulomb attraction accomodates an "inner" ground state with a too large absorption width.

The π^- bound states belong to a new family of nuclear excited states. For instance, the π^- ^{208}Pb bound states are excited states of $^{208}T\ell$ with "pionic" quantum numbers (unnatural-parity states: 0^-, 1^+, 2^-, $\cdots$), as shown in Fig.7. How can we produce and identify those states? We will discuss this problem below.

3. FORMATION OF PIONIC STATES

Since deeply bound π^- states belong to a special family of nuclear excied states, as shown in Fig.7, they can be populated by various ways, as Toki and Yamazaki discussed [16]. The π^- bound states of orbitals of s, p, d, f, *etc.* are characterized by "unnatural" spins and parities, *i.e.*, 0^-, 1^+, 2^-, 3^+, *etc.* The transitions from ^{208}Pb to π^- ^{208}Pb are of the Gamow-Teller type, namely, $\Delta S = 1$ and $\Delta T = 1$. Thus, the new family of pionic bound states is a new kind of Gamow-Teller resonances. In the following we will review various ways for the formation of pionic bound states.

A) Charge-exchange pion-transfer reactions

Toki and Yamazaki [16] proposed to populate them by the (n,p) reaction. because it is the most natural way to produce a π^- through the Yukawa vertex n $\to$ p + π^-. This vertex does not take place in free spece, but can produce a π^- to be embedded in a target nucleus, as shown in Fig. 8a. This process may be called "pion-transfer" reaction, where the virtual pion in the incoming neutron is transferred to a "real pion" bound state.

Toki *et al.* [16,17] calculated the (n,p) cross sections based on the plane-wave impulse approximation (PWIA). The cross section is presented by

$$\left[\frac{d\sigma}{d\Omega}\right]_{(n,p)} = \frac{M^2}{(2\pi)^2}\frac{p_f}{p_i}\left(\frac{f}{m_\pi}\right)^2\frac{q_L^2}{m_\pi}\sum_m |\Psi_{n\ell m}(q)|^2 \quad (4)$$

where p_i and p_f are the momenta of the incoming neutron and the outgoing proton, respectively, the momentum transfer $\vec{q} = \vec{p}_i - \vec{p}_f$ is given by

$$\begin{aligned} q &= \omega\frac{E_i}{p_i}\frac{1}{\cos\theta_{rec}} \\ \tan\theta &= \frac{q\sin\theta_{rec}}{p_i - q\cos\theta_{rec}}, \\ \tan\theta_{rec} &= \frac{p_f\sin\theta}{\pi - p_f\cos\theta} \end{aligned} \quad (5)$$

and the Lorentz-invariant momentum transfer q_L is

$$q_L^2 = (p_i - p_f)^2 - (E_i - E_f)^2$$
$$= q^2 - \omega^2 \tag{6}$$

The typical momentum transfer at 0 degree with $T_n = 400$ MeV is $q = 200$ MeV/c and the q_L is 140 MeV/c. The cross section is proportional to the square of the Fourier transform of the pion wavefunction. For deeply bound π^- states the Fourier components at $q = 200$ MeV/c are quite sizable. The calculated spectrum for ^{208}Pb (n,p) π^- ^{208}Pb is shown in Fig.9, where the calculated cross sections are reduced by a factor of 10 in view of the possible distortion effect. The background cross section is taken to be 0.8 mb/sr/MeV.

The distortion effect was calculated by Toki [19], who gave reduction factors of 1 ~ 10% for the cross section, depending on the state formed. Nieves and Oset [20] considered other diagrams (NN $\rightarrow$NNπ) as well.

B) Proton-pick up pion-transfer reaction

Toki and Yamazaki [16] discussed to use (n,d), (p,^{2}He) or (d,^{3}He), where one neutron in configuration j_n is picked up as a proton added to the projectile, leaving a π^- in the target to form a π^- state $n\ell$ on a neutron-hole state ϕ_{j_n}. The elementary process is

$$Nn \rightarrow Np\pi^-, \tag{7}$$

where N is the projectile nucleon (see diagrams in Fig.6). Using the known elementary cross section they evaluated the formation cross section as follows,

$$\frac{d\sigma}{d\Omega} = \left(\frac{d\sigma}{d\Omega}\right)^{\rm lab}_{(n+n\rightarrow d+\pi^-)} \mid \int \Phi^*_{n\ell}(\vec{r})\ exp\left[-i(\vec{k}_d - \vec{k}_n)\vec{r}\right] \phi_{j_n}(\vec{r}) d^3r \mid^2 . \tag{8}$$

This reaction has a relatively low momentum transfer, $q = k_n - k_d$, typically, 70, 130, 170 and 210 MeV/c for $T_n = 400, 500, 600$ and 700 MeV, respectively, and the reaction amplitude depends on the overlapping between the pionic wavefunction and the neutron-hole state. The residual state has configuration $(j_n^{-1}\ell_\pi)_{JL}$. As in hypernuclear spectroscopy, a fully occupied large-j_n orbital contributes dominantly to the formation of $(j_n^{-1}\ell_\pi)$ states. In the case of ^{208}Pb the $i_{13/2}$ orbital is important. A suitable momentum transfer helps the necessary angular momentum transfer in the reaction.

A realistic calculation of Toki et al. [19] gives the following cross sections;

$$\left(\frac{d\sigma}{d\Omega}\right)_{(n,d\pi^-)} = \left(\frac{d\sigma}{d\Omega}\right)^{\rm lab}_{(nn\rightarrow d\pi^-)} N_{\rm eff}, \tag{9}$$

where

$$N_{\rm eff} = \frac{1}{2}\sum_{\ell m} \mid S\sqrt{\frac{2J+1}{2\ell_\pi+1}}(-)^{\ell n}\frac{(2\ell_\pi+1)(2\ell_n+1)}{4\pi(2L+1)}(\ell_\pi 0\ \ell_n 0 \mid L0)$$
$$\times (-)^{\ell n} 4\pi \int j_L(qr)D(r)R_\pi(r)R_n(r)r^2 dr \mid^2, \tag{10}$$

where S is a statistial factor and $D(r)$ is a distortion coefficient.

For $\ell_\pi = 0$ (1s state) and $j_n = i_{13/2}$,

$$N_{\rm eff} = \begin{cases} 1.5 \times 10^{-2} & \text{(plane wave)} \\ 2.8 \times 10^{-3} & \text{(distorted wave).} \end{cases}$$

The cross sections at $T_n = 600$ MeV is estimated to be

$$\left(\frac{d\sigma}{d\Omega}\right)_{(n,d\pi^-)} = \begin{cases} 30\ \mu\text{b/sr} & \text{(plane wave)} \\ 56\ \mu\text{b/sr} & \text{(distorted wave).} \end{cases}$$

The distorted wave cross section for the 2p-state formation is 6.0 and 3.6 μ/sr for $J = 15/2$ and $11/2$, respectively, but very small for $J = 13/2$.

This reaction is different from the pion-transfer reaction in the sense that the target nucleus is changed into a neutron-hole state. The neutron hole distributes over many states, and the formation of the ground state is only a part. The situation is similar to the hypernuclear formation in strange-exchange reactions. However, in the case of ^{208}Pb target, the $i_{13/2}$ hole dominates the reaction amplitude. The momentum transfer of the (d, ^{3}He) reaction, $q \sim 200$ MeV/c for $T_d \sim 1$ GeV, matches the angular momentum transfer of $6\hbar$.

It is interesting to examine the fine structure of $(j_n^{-1}\ell_\pi)_J$ multiplets, as it will yield useful information on the spatial distribution of the j_n neutron hole and the π^-- neutron residual interaction.

The second method of this category is to use (e,e'p) or (γ, p) reactions, as discussed by Tzara [21], Dimitriev [22] and Koch [23]. The Nn→Npπ^- vertex above is replaced by the γn→pπ^- vertex (see diagrams in Fig.8b).

How can we excite pionic bound states by (p,p')? The reaction diagram is similar to the (p, 2p) reaction, but one of the outgoing proton should stay to form a particle-hole state $(j_n^{-1}j_p)\ell_\pi$, and so the cross section is small and the final state is more complicated. For instance, the ^{208}Pb(p,p') reaction produces π^- ^{208}Bi. The low-lying states of ^{208}Bi are too complicated for the spectroscopy of deeply bound π^- states.

C) *Resonance Formation*

The resonance formation of pionic states is possible with various projectiles, as shown in Fig.8c. A method to use the proton-capture reaction was proposed by Emery [24]. The cross section for the formation of a resonant pionic state $n\ell$ with a total width $\Gamma_{n\ell}$ by a proton-caption reaction is given by

$$\sigma_{n\ell}(E) = \frac{\lambda_p^2}{\pi}\frac{2J_f+1}{2(2J_i+1)}\frac{\Gamma_{n\ell}^p}{\Gamma_{n\ell}}\frac{\Gamma_{n\ell}^2}{(E-E_{n\ell})^2+\Gamma_{n\ell}^2} \tag{11}$$

The cross section depends on the partial width $\Gamma_{n\ell}^p$. The main decay channel of π^- bound states, $\pi^-pn \rightarrow nn$, does not contribute to $\Gamma_{n\ell}^p$. The $\Gamma_{n\ell}^p$, partial width for the ground state of the target nucleus, is only a very small portion of the less likely channel π^-pp → pn. Furthermore, the final state has a complicated configuration $j_n^{-1}j_pj_p'\ell_\pi$.

The neutron-capture reaction is more favourable than the proton-capture reaction, because the π^-pn → nn channel is dominating and furthermore it forms pionic states of simpler contiguration, namely, on a proton-particle contiguration $(j_p\ell_\pi)$. For this purpose a high-resolution beam of about 140 MeV is needed.

The momentum transfer in the resonance formation of pionic states with nucleon capture is about 500 MeV/c. This momentum transfer is too large even when a large anglar momentum in the formation of proton-particle state $(j_p\ell_\pi)$ is taken into account.

The resonance formation of pionic states with a monochromatic photon beam is possible, where the final state has a configuration $(j_n^{-1}j_p\ell_\pi)$. The momentum transfer is 140 MeV/c, which is matched to the angular momentum transfer.

D) Other methods

Very recently Nieves and Oset [25] proposed to use the (γ, π^+) reaction to populate pionic bound states. This reaction does not change the nuclear state, thus giving "coherent production" as well as the (n,p) reaction. The peak cross section at $E_\gamma = 455$ MeV is 0.025 and 0.050 μb/sr/MeV for the 1s and 2p states, respectively.

Gridnev [26] proposed the (π^-, p) reaction. This is a kind of knock-on reaction similar to ($\bar{p}$, p) proposed by Gibbs and Kaufman [27] for the formation of anti-protonic bound states. The cross sections are sizable.

4. EXPERIMENTS ON CHARGE-EXCHANGE REACTIONS

An experiment to search for discrete peaks in the ^{208}Pb(n,p) ^{208}Tℓ reaction was carried out by using the monoenergetic neutrons of 420 MeV from the TRIUMF CHARGEX facility [28]. Monoenergetic neutrons obtained from the ^{7}Li(p,n) ^{7}Be reaction induced by 420 MeV protons were introduced to a ^{208}Pb target assembly and the (n,p) proton spectrum was measured with the Medium Resolution Spectrometer [29]. The overall energy resolution was obtained to be 1.15 MeV. The result is shown in Fig.10. This spectrum shows a smooth continuous behavior with a cross section of 0.8 mb/sr/MeV. The PWIA estimate is shown in the inset. Clearly, the experimental data is in disagreement with this estimate. An upper limit of 0.35 mb/sr for a peak was obtained. This limit indicates that the peak cross section is certainly less than the PWIA estimate, but allows the reduction factor to be less than 0.3.

The TRIUMF experiment suffered from insufficient statistics and large background, because a secondary neutron beam is used. An alternative way is to use the (d,^{2}He) reaction. At SATURNE of Saclay this reaction at intermediate energy was measured with the SPES4 spectrometer system to study both Gamow-Teller resonances and Δ excitation [30]. The region of present interest lies in a valley between the low energy GT/quasi-free region and the Δ resonance region. A search

experiment was planned and carried out [31,32]. The (d,^{2}He) experiment will not only yield a much better statistics than the (n,p) experiment but also make use of the polarization enhancement. As far as the pion transfer is described by the longitudinal operator $\vec{\sigma} \cdot \vec{q}$, the transversely polarized deutron beam enhances the cross section by a factor of 3 [32]. The SATURNE experiment is capable for detecting the formation of deeply bound π^- states, if the cross section is larger than 0.1 mb/sr. The overall energy resolution is expected to be 0.6 MeV FWHM.

5. HEAVY-ION REACTIONS WITH INVERSE KINEMATICS

Since the natural widths of pion-bound states are of the order of 10-100 keV, it would be ideal, if one could attain a high resolution, say, 10 keV, but it is difficult to achieve such an energy resolution with the conventional charge-exchange reactions.

Recently, Yamazaki *et al.* [33] proposed a new type of experiment using the inverse kinematics with an intermediate-energy heavy-ion beam, where a cooled ^{208}Pb beam of kinetic energy of 400 MeV/u hits a light target such as d and t, and recoil particles such as ^{2}He and ^{3}He are detected. The momentum of recoil particle is calculated as a function of the excitation energy ω (or the Q value), as shown in Fig.11. It was shown that the recoil momentum is nearly equal to the Lorentz-invariant momentum transfer q_L, eq.(6). The accuracy of excitation energy depends on the accuracy in the determination of recoil angle. Both the momentum and its direction of recoil particle have to be precisely determined.

Some experimental configurations are proposed, as shown in Fig.12. It is possible to attain the energy resolution as good as 50 keV. The expected recoil spectra corresponding to the (n,p) spectrum of Fig.9 are shown in Fig.13. Such an experiment seems to be feasible with the new heavy-ion synchrotron/cooler ring SIS/ESR of GSI.

Acknowledgement

The present paper is dedicated to the 60th birthday of Professor Torleif Ericson. The author would like to thank Professor Ericson for the stimulating discussions and encouragement. He is very much indebted to many colleagues, in particular, Professor H. Toki and R.S. Hayano. The work is partially supported by the International Scientific Research Program of Japanese Ministry of Education, Science and Culture.

REFERENCES

[1] M. Krell and T.E.O. Ericson, Nucl. Phys. B11 (1969) 521.

[2] M. Ericson and T.E.O. Ericson, Ann. Phys. 36 (1966) 323.

[3] R. Seki and K. Masutani, Phys. Rev. C27 (1983) 2799.

[4] R. Rockmore, Phys. Letters B205 (1988) 179.

[5] R. Seki, Prog. Theor. Phys. 74 (1985) 511.

[6] R.S. Hayano, T. Ishikawa, M. Iwasaki, H. Outa, E. Takada, H. Tamura, A. Sakaguchi, M. Aoki and T. Yamazaki Phys. Letters B231 (1989) 355.

[7] T. Harada, S. Shinmura, Y. Akaishi and H. Tanaka, Nucl. Phys. A507 (1990) 715.

[8] T. Yamazaki, R.S. Hayano, O. Morimatsu and K. Yazaki, Phys. Letters B207 (1988) 393.

[9] Khin Swe Myint, S. Tadokoro and Y. Akaishi, Prog. Theor. Phys. 82 (1989) 112.

[10] T. Yamazaki, M. Aoki, Y. Fujita, R.S. Hayano, H. Tamura, T. Ishikawa, E. Takada, M. Iwasaki, H. Outa, J. Imazato and A. Sakaguchi, Nuovo Cimento 102A (1989) 695.

[11] See, for instance, K. Ikeda, Proc. 5th International Conf. on Clustering Aspects in Nuclear and Subnuclear Systems (ed. K. Ikeda, K. Katori and Y. Suzuki, Phys. Soc. Japan, 1988) p.277.

[12] T. Yamazaki, in "Perspectives of Particle Physics" (ed. S. Matsuda, T. Muta and R. Sasaki, World Scientific, Singapore, 1989) p.44.

[13] Y. Nambu and G. Jona-Lasinio, Phys. Rev. 122 (1961) 345; 124 (1961) 246.

[14] T. Yamazaki, Phys. Letters B160 (1985) 227.

[15] J.J. Aubert *et al.*, Phys. Letters B123 (1983) 275; A. Bodek *et al.*, Phys. Rev. Letters 50 (1983) 1431; 51 (1983) 534.

[16] H. Toki and T. Yamazaki, Phys. Letters B213 (1988) 129.

[17] H. Toki, S. Hirenzaki, T. Yamazaki and R.S. Hayano, Nucl. Phys. A501 (1989) 653.

[18] E. Friedman and G. Soff, J. Phys. G11 (1985) L37.

[19] H. Toki, private communication (1990).

[20] J. Nieves and E. Oset, preprint (1990).

[21] C. Tzara, Nucl. Phys. B18 (1970) 246.

[22] U.F. Dimitriev, Sov. J. Nucl. Phys. 17 (1973) 417.

[23] J.H. Koch, Phys. Letters B59 (1975) 45.

[24] G.T. Emery, Phys. Letters B60 (1976) 351.

[25] J. Nieves and E. Oset, preprint (1990).

[26] A.B. Gridnev, private communication (1990).

[27] W.R. Gibbs and W.B. Kaufman, Phys. Letters B145 (1984) 1.

[28] M. Iwasaki *et al.*, to be published.

[29] K.P. Jackson *et al.*, Phys. Letters B206 (1988) 597.

[30] C. Ellegaard *et al.*, Phys. Rev. Letters 59 (1987) 974.

[31] T. Yamazaki and P. Radvanyi (spokesman), SATURNE proposal No.214 (December, 1988).

[32] T. Yamazaki, Proc. 5th French-Japanese Symposium on Nuclear Physics, Dogashima, 1989 (ed. K. Shimizu and O. Hashimoto) p.309.

[33] T. Yamazaki, R.S. Hayano, H. Toki and P. Kienle, Nucl. Instr. Meth., in press.

FIGURE CAPTIONS

Fig.1 Pion spectra from ^{4}He(stopped K^-,π^-), $^4_\Sigma$He (left) and ^{4}He (stopped K^-, π^+)$^4_{\Sigma^-}n$ (right) showing the presence of a bound state in $^4_\Sigma$He, but not in $^4_{\Sigma^-}$n. From Hayano *et al.* [6].

Fig.2 The realistic Σ-nucleus potential and the Σ density (solid curves) as compared with the conventional ones (broken curves), calculated by Harada *et al.* [7]. The dotted curve is for the imaginary part.

Fig.3 Σ^- nuclei as Coulomb-assisted hybrid bound states.

Fig.4 Generalized diagram of nuclear excited states in terms of "particle cluster".

Fig.5 Level structure of π^- in ^{90}Zr and ^{208}Pb.

Fig.6 Pion potential and pion densities in π^{-208}Pb.

Fig.7 Pionic excited states as a special Gamow-Teller family of nuclear excited states.

Fig.8 Various diagrams for the formation of pionic states.

Fig.9 Expected spectrum of pionic state formation in the ^{208}Pb(n,p)^{208}Tℓ reaction at T_n = 400 MeV. The cross sections are assumed to be 1/10 of the PW estimates.

Fig.10 Observed spectrum of the ^{208}Pb(n,p)^{208}Tℓ reaction at T_n = 420 MeV, from a recent TRIUMF experiment using a monoenergetic neutron beam [28].

Fig.11 Kinematical relation in the inverse kinematics. The recoil momentum vs the excitation energy for a given laboratory emission angle.

Fig.12 An example of the detection system for the measurement of the recoil momentum and its direction [33].

Fig.13 Expected recoil spectrum assuming the (n,p) spectrum as given in Fig. 9, taken from Ref. [33].

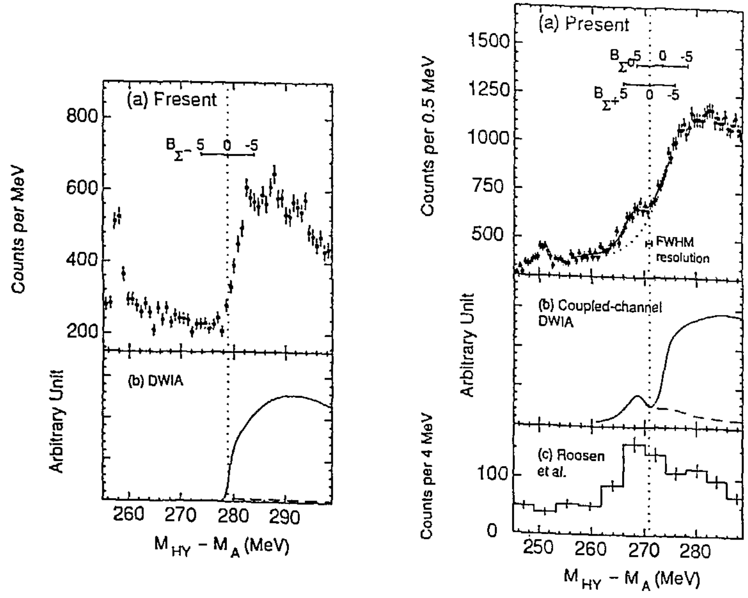
(a) Present
B_{Σ^-} 5 0 -5
Counts per MeV
800
600
400
200
(b) DWIA
Arbitrary Unit
260
270
280
290
$M_{HY} - M_A$ (MeV)
(a) Present
B_{Σ^0} 5 0 -5
B_{Σ^+} 5 0 -5
Counts per 0.5 MeV
1500
1250
1000
750
500
FWHM resolution
(b) Coupled-channel DWIA
Arbitrary Unit
(c) Roosen et al.
Counts per 4 MeV
100
0
250
260
270
280
$M_{HY} - M_A$ (MeV)

Fig. 1

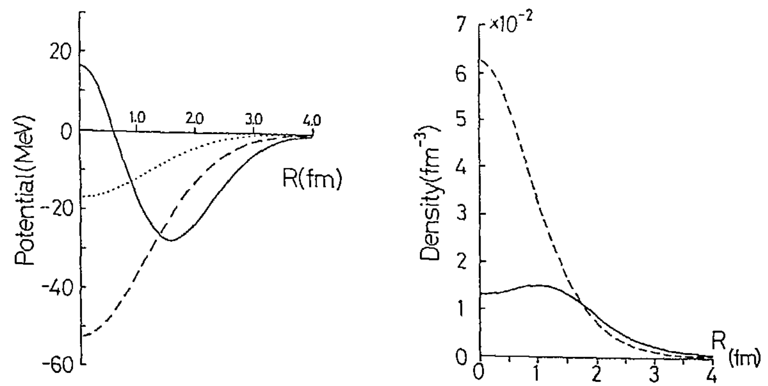
Potential(MeV)
20
0
-20
-40
-60
1.0
2.0
3.0
4.0
R(fm)
Density(fm^{-3})
$\times 10^{-2}$
7
6
5
4
3
2
1
0
0
1
2
3
4
R (fm)

Fig. 2

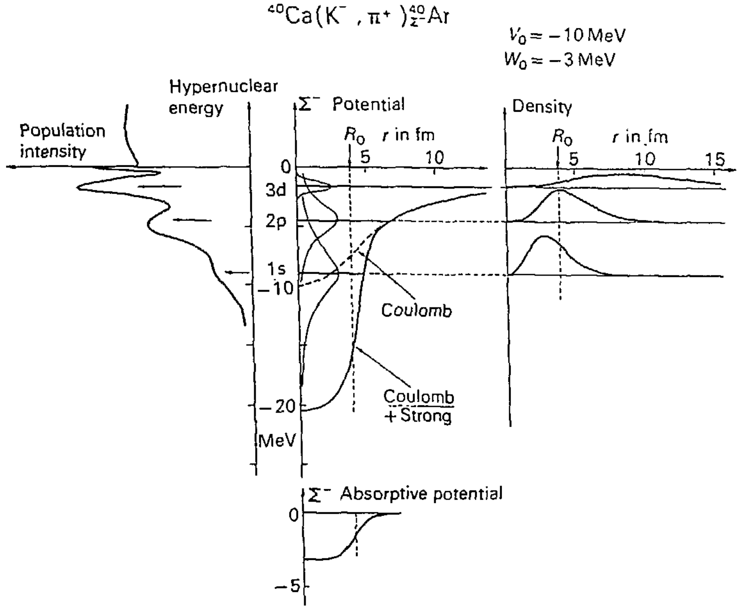

⁴⁰Ca(K⁻, π⁺)⁴⁰Ar
V₀ = −10 MeV
W₀ = −3 MeV
Hypernuclear energy
Population intensity
Σ⁻ Potential
Density
R₀
r in fm
0
5
10
15
3d
2p
1s
−10
−20
MeV
Coulomb
Coulomb + Strong
Σ⁻ Absorptive potential
−5

Fig. 3

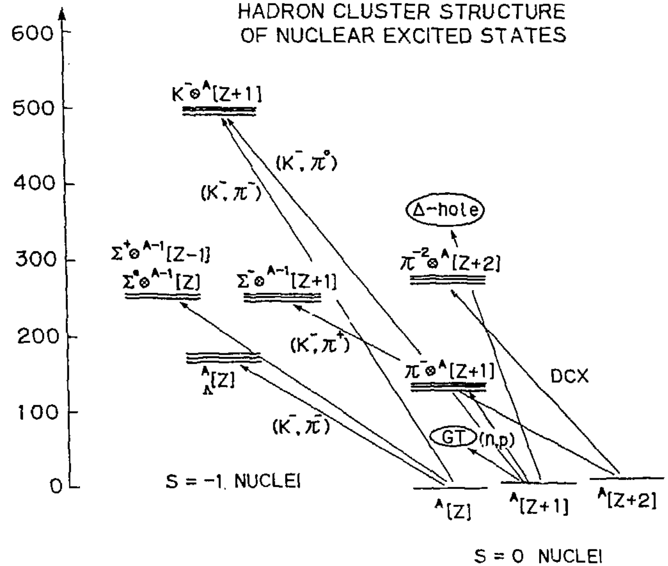

HADRON CLUSTER STRUCTURE
OF NUCLEAR EXCITED STATES
600
500
400
300
200
100
0
K⁻⊗ᴬ[Z+1]
(K⁻, π⁰)
(K⁻, π⁻)
Δ-hole
Σ⁺⊗ᴬ⁻¹[Z−1]
Σ⁰⊗ᴬ⁻¹[Z]
Σ⁻⊗ᴬ⁻¹[Z+1]
π⁻²⊗ᴬ[Z+2]
(K⁻, π⁺)
π⁻⊗ᴬ[Z+1]
DCX
ᴬΛ[Z]
(K⁻, π⁻)
GT
(n,p)
S = −1 NUCLEI
ᴬ[Z]
ᴬ[Z+1]
ᴬ[Z+2]
S = 0 NUCLEI

Fig. 4

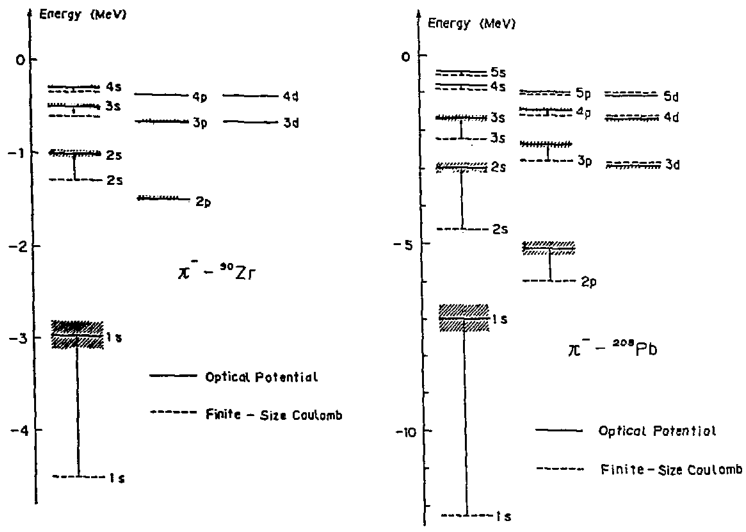
Energy (MeV)
0
-1
-2
-3
-4
4s
3s
2s
1s
4p
3p
2p
4d
3d
π^- - ^{90}Zr
Optical Potential
Finite - Size Coulomb
Energy (MeV)
0
-5
-10
5s
4s
3s
2s
1s
5p
4p
3p
2p
5d
4d
3d
π^- - ^{208}Pb
Optical Potential
Finite - Size Coulomb

Fig. 5

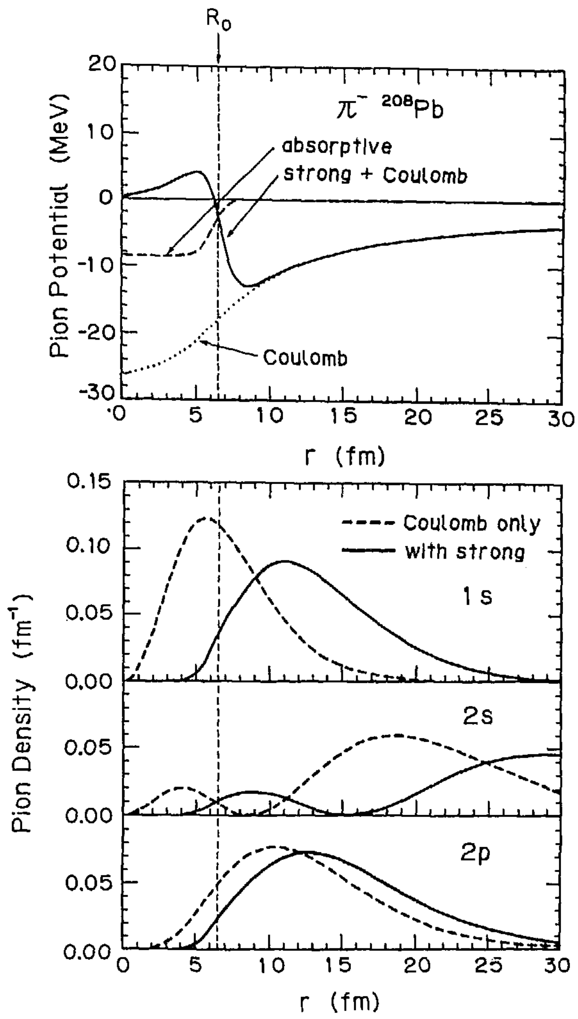
R$_0$
π^- ^{208}Pb
absorptive
strong + Coulomb
Coulomb
Pion Potential (MeV)
r (fm)
Coulomb only
with strong
1s
2s
2p
Pion Density (fm^{-1})
r (fm)

Fig. 6

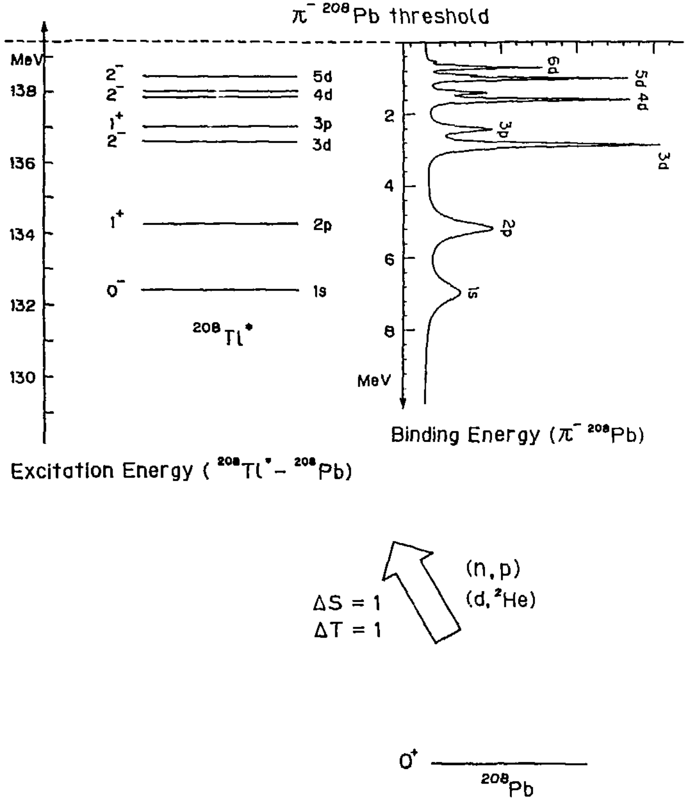

π⁻ 208Pb threshold
MeV
138
136
134
132
130
2⁻ 5d
2⁻ 4d
1⁺ 3p
2⁻ 3d
1⁺ 2p
0⁻ 1s
208Tl*
2
4
6
8
MeV
6d
5d 4d
3p
3d
2p
1s
Binding Energy (π⁻ 208Pb)
Excitation Energy (208Tl* − 208Pb)
(n, p)
(d, 2He)
ΔS = 1
ΔT = 1
0⁺
208Pb

Fig. 7

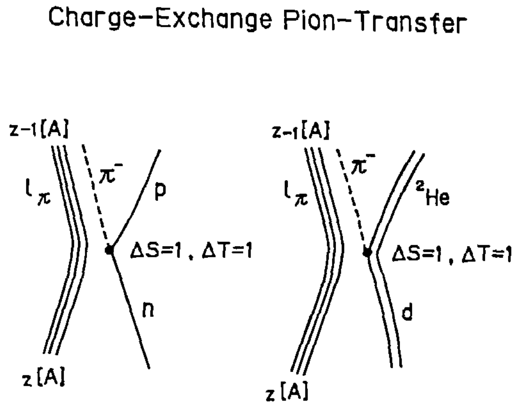

Charge-Exchange Pion-Transfer
z-1[A]
lπ
π⁻
p
ΔS=1, ΔT=1
n
z[A]
z-1[A]
lπ
π⁻
2He
ΔS=1, ΔT=1
d
z[A]

Fig. 8 (a)

Proton-Pickup Pion-Transfer

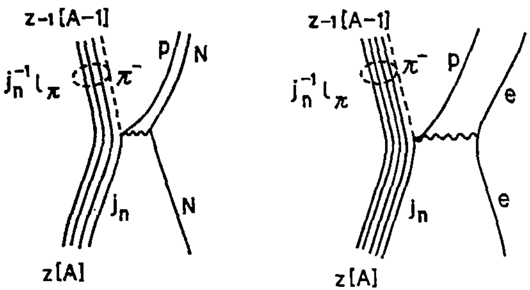

Fig. 8 (b)

Resonant Formation

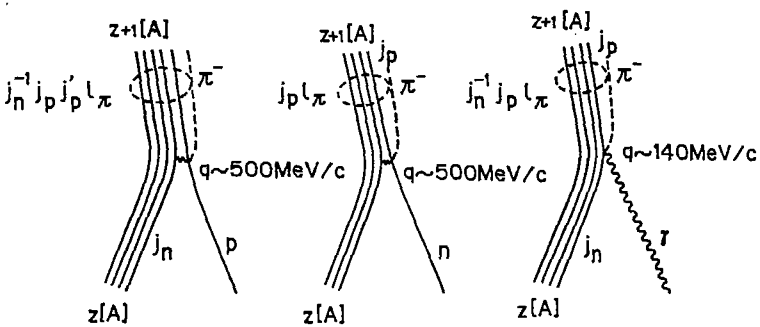

Fig. 8 (c)

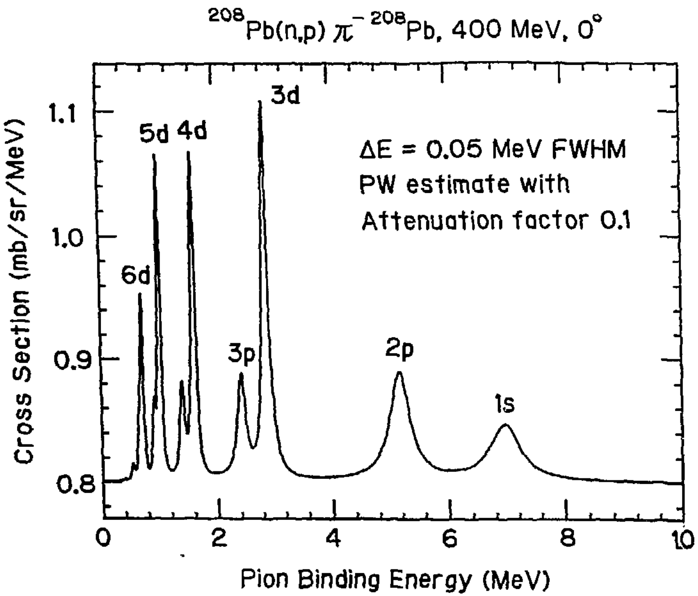

^{208}Pb(n,p) π^{-} ^{208}Pb, 400 MeV, 0°
ΔE = 0.05 MeV FWHM
PW estimate with
Attenuation factor 0.1
6d
5d
4d
3d
3p
2p
1s
Cross Section (mb/sr/MeV)
Pion Binding Energy (MeV)

Fig. 9

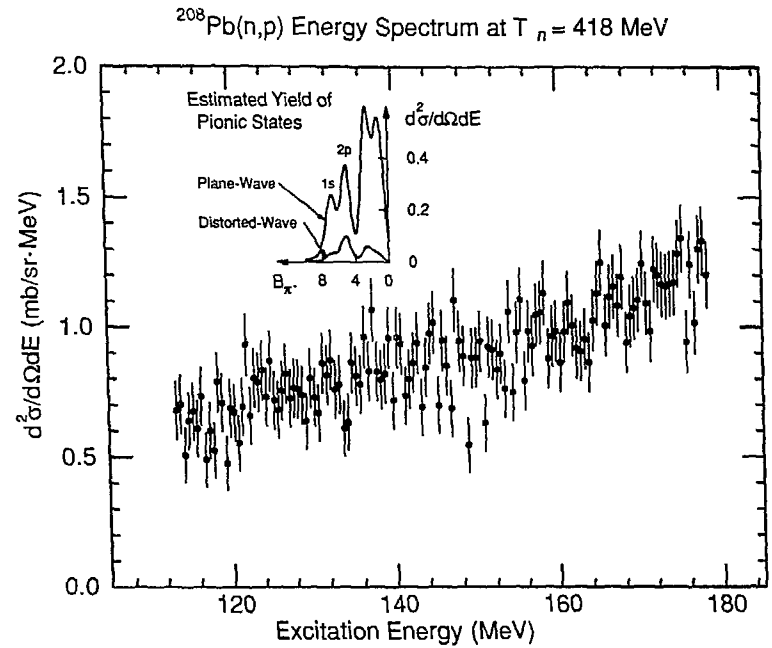

^{208}Pb(n,p) Energy Spectrum at T $_n$ = 418 MeV
Estimated Yield of
Pionic States
Plane-Wave
Distorted-Wave
$d^2\sigma/d\Omega dE$
$d^2\sigma/d\Omega dE$ (mb/sr·MeV)
Excitation Energy (MeV)

Fig. 10

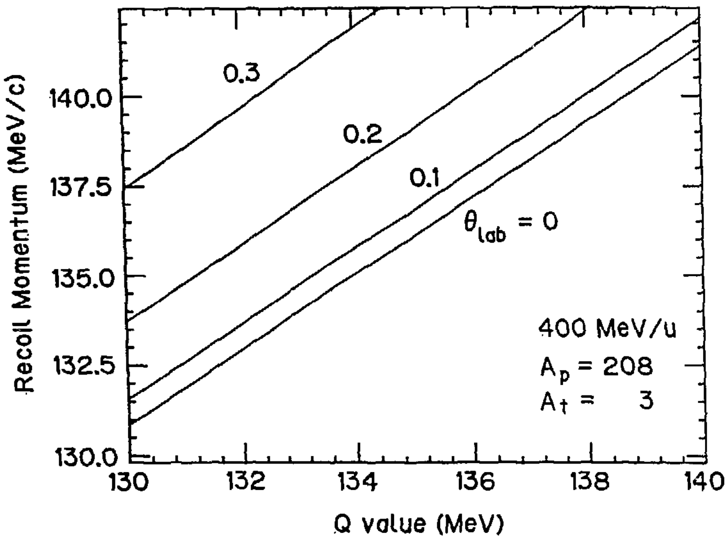

Recoil Momentum (MeV/c)
140.0
137.5
135.0
132.5
130.0
130
132
134
136
138
140
Q value (MeV)
0.3
0.2
0.1
θlab = 0
400 MeV/u
Ap = 208
At = 3

Fig. 11

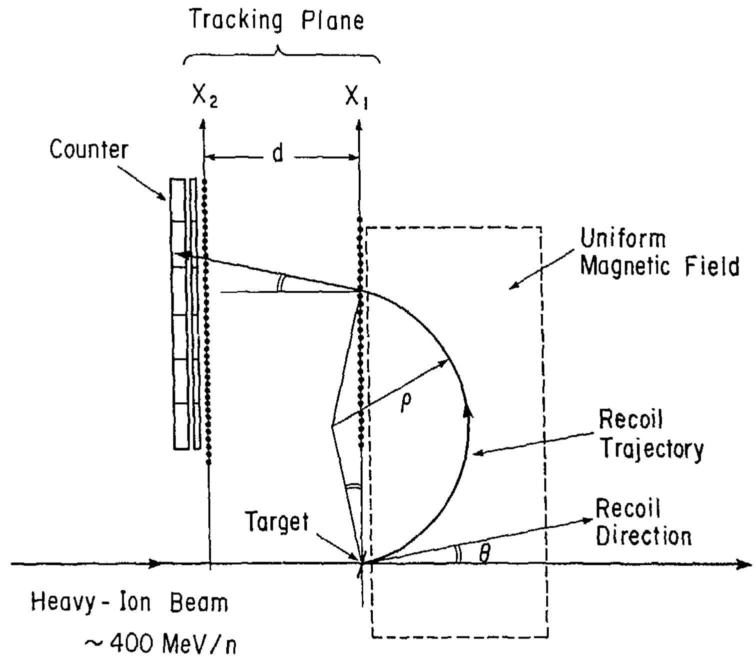

Tracking Plane
X2
X1
Counter
d
Uniform
Magnetic Field
ρ
Recoil
Trajectory
Target
Recoil
Direction
θ
Heavy - Ion Beam
~ 400 MeV/n

Fig. 12

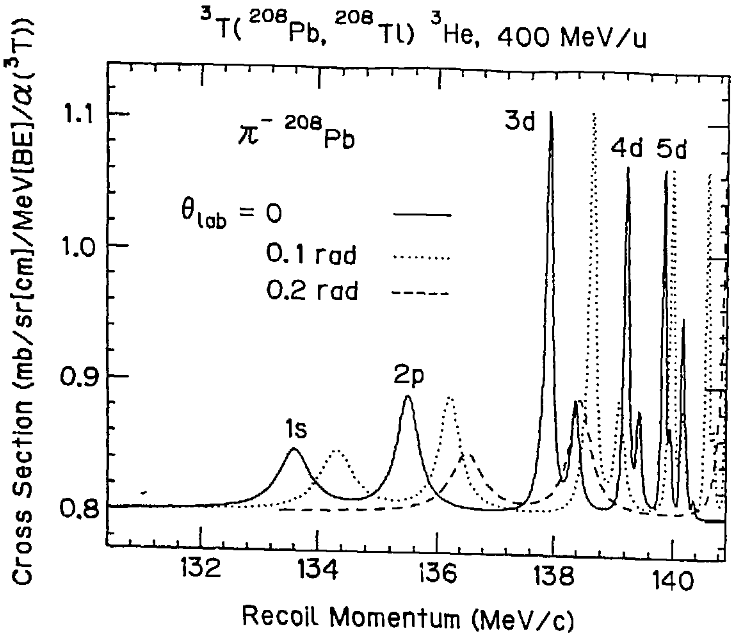

$^3T(^{208}Pb, ^{208}Tl)\ ^3He$, 400 MeV/u
$\pi^{-}\ ^{208}Pb$
θ_{lab} = 0
0.1 rad
0.2 rad
1s
2p
3d
4d
5d
1.1
1.0
0.9
0.8
132
134
136
138
140
Recoil Momentum (MeV/c)
Cross Section (mb/sr[cm]/MeV[BE]/$\alpha(^3T)$)

Fig. 13